calibrated for LEWICE but does not play an identical role in the S–A model as in an integral method. However, although the two approaches are quite different, their solutions agree pretty much, and the results are satisfactory. In this test case, on the clean airfoil, the impingement solution of DROP3D and ICE3D are identical (Ref. 8). In Fig. 3b, the LEWICE numerical solution obtained after 1 min of accretion is compared to the ICE3D solution, and they agree pretty well. The small differences between the convective heat flux coefficients of LEWICE and FENSAP S–A do not significantly influence the ice shape and, thus, confirm the validity of our convective heat fluxes and validate our PDE-based icing approach.

Conclusions

The one-equation S–A turbulence model has been implemented in the three-dimensional FEM flow solver, FENSAP, of the FENSAP-ICE in-flight icing simulation system. The surface roughness of iced surfaces has been taken into account with an equivalent sand grain roughness parameter. The effects of roughness on the flow solution have been successfully validated against numerical and experimental results, and the roughness effects on ice shapes have been demonstrated through a NACA 0012 wing test case. The S–A model has proven to be robust, to be easy to use, and showed good agreement with theory and experiments, making it a valuable tool for PDE-based in-flight icing simulations.

Acknowledgment

We would like to thank Philippe Spalart of The Boeing Company for his advice in implementing the roughness within his turbulence model.

References

[1]Bourgault, Y., Habashi, W. G., Dompierre, J., and Baruzzi, G. S., "A Finite Element Method Study of Eulerian Droplets Impingement Models," *International Journal for Numerical Methods in Fluids*, Vol. 29, 1999, pp. 429–449.

[2]Beaugendre, H., Morency, F., and Habashi, W. G., "ICE3D, FENSAP-ICE's In-flight Ice Accretion Module," *Proceedings of the 48th CASI Annual Conference*, Canadian Aeronautics and Space Inst., Toronto, 2001, pp. 271–276.

[3]Spalart, P. R., and Allmaras, S. R., "A One-Equation Turbulence Model for Aerodynamic Flows," AIAA Paper 92-0439, Jan. 1992.

[4]Remaki, L., Beaugendre, H., and Habashi, W. G., "ISOD—An Anisotropic Isovalue-Oriented Diffusion Artificial Viscosity for the Euler and Navier-Stokes Equations," *Journal of Computational Physics*, Vol. 186, No. 1, 2003, pp. 279–294.

[5]Gresho, P. M., Lee, R. L., Sani, R. L., Maslanik, M. K., and Eaton, B. E., "The Consistent Galerkin FEM for Computing Derived Boundary Quantities in Thermal and/or Fluid Problems," *International Journal for Numerical Methods in Fluids*, Vol. 7, No. 4, 1987, pp. 371–394.

[6]Spalart, P. R., "Trends in Turbulence Treatments," AIAA Paper 2000-2306, Jan. 2000.

[7]Hellsten, A., and Laine, S., "Extension of the k–ω-SST Turbulence Model for Flows over Rough Surfaces," AIAA Paper 97-3577, Jan. 1997.

[8]Beaugendre, H., "A PDE-Based 3D Approach for In-Flight Ice Accretion," Ph.D. Dissertation, McGill Univ., Montreal, QC, Canada, June 2003.

[9]Blanchard, A., "Analyse Expérimentale et Théorique de la Structure de la Turbulence d'une Couche Limite sur Paroi Rugueuse," Ph.D. Dissertation, Unite d'Enseignement et de Recherche-Ecole Nationale Superieure de Mecanique et d'Aerotechnique, Univ. de Poitiers, Poitiers, France, May 1977.

[10]Aupoix, B., and Spalart, P. R., "Extensions of the Spalart–Allmaras Turbulence Model to Account for Wall Roughness," *International Journal of Heat and Fluid Flow*, Vol. 24, No. 4, Aug. 2003, pp. 454–462.

[11]Wright, W. B., and Rutkowski, A., "Validation Results for LEWICE 2.0," [CD-ROM], NASA CR-1999 203690, Jan. 1999.

Benefit and Performance of Various Vortex Flap Configurations

Kenichi Rinoie*
University of Tokyo, Tokyo 113-8656, Japan

Introduction

THE leading-edge vortex flap (LEVF) is one of the devices that can improve the aerodynamic efficiency of delta wings at low speeds.[1] The LEVF is a full-span deflectable flap attached to the leading edge of the delta wing. With the flap deflected downward, a leading-edge separation vortex can be formed over the forward-facing flap surface. The vortex suction force acting normal to the flap surface generates a thrust component. Hence, this leading-edge suction reduces the drag of the wing and improves the lift/drag ratio at a given lift coefficient. Reference 2 contains an overview of LEVF research. Many tests have been done that confirm the benefit of the LEVF.[3,4] It has also been pointed out that LEVFs are effective for reduction of takeoff noise associated with the low-speed inefficiency of the delta wing used for the supersonic transport.[5]

It is clear that the vortex flap deflection angle is an important factor that determines the formation of the leading-edge separation vortex on the flap surface and the improvements of the lift/drag ratio of the delta wing. There are other factors that affect the vortex flap characteristics: 1) sweepback angle, 2) area ratio of the LEVFs/the delta wing, and 3) leading-edge shapes, that is, sharp or rounded leading edges. The sweepback angle determines the original delta wing aerodynamic characteristics, and hence, the performance of the LEVFs will also be affected. The area of the vortex flaps also affects the formation of the leading-edge separation vortex on the flap surface. As for leading-edge shapes, by deflecting the rounded LEVF, suction forces, which are caused both by the leading-edge separation vortex over the flap surface and by the rounded leading edge, may reduce the drag component and increase the lift/drag ratio.

Several experimental studies have been conducted using delta wing models with tapered vortex flaps that have different sweepback angles,[6–8] different flap areas,[9] and different leading-edge shapes.[10] The aim of this note is to discuss and summarize the benefit of vortex flaps that have different configurations, by reviewing the experimental results obtained by the author and others.

Experimental Details

The plan shape of the vortex flap is mainly classified into two different types. First is the flap that has a constant chord length along the whole part of the wing span. Many studies have investigated this type of vortex flap.[1,11] Another type is a tapered vortex flap. Figure 1 shows a schematic diagram of the tapered vortex flaps. The delta wing has vortex flap hinge lines running from the wing apex to the trailing edge. The vortex flap deflection angle δ_f is defined as the angle measured in the plane normal to the hinge line. The flap hinge-line position fr is defined as

$$fr = h/(b/2) \tag{1}$$

Received 21 July 2003; accepted for publication 25 July 2003.

*Associate Professor, Department of Aeronautics and Astronautics, 7-3-1 Hongo, Bunkyo-ku. Senior Member AIAA.

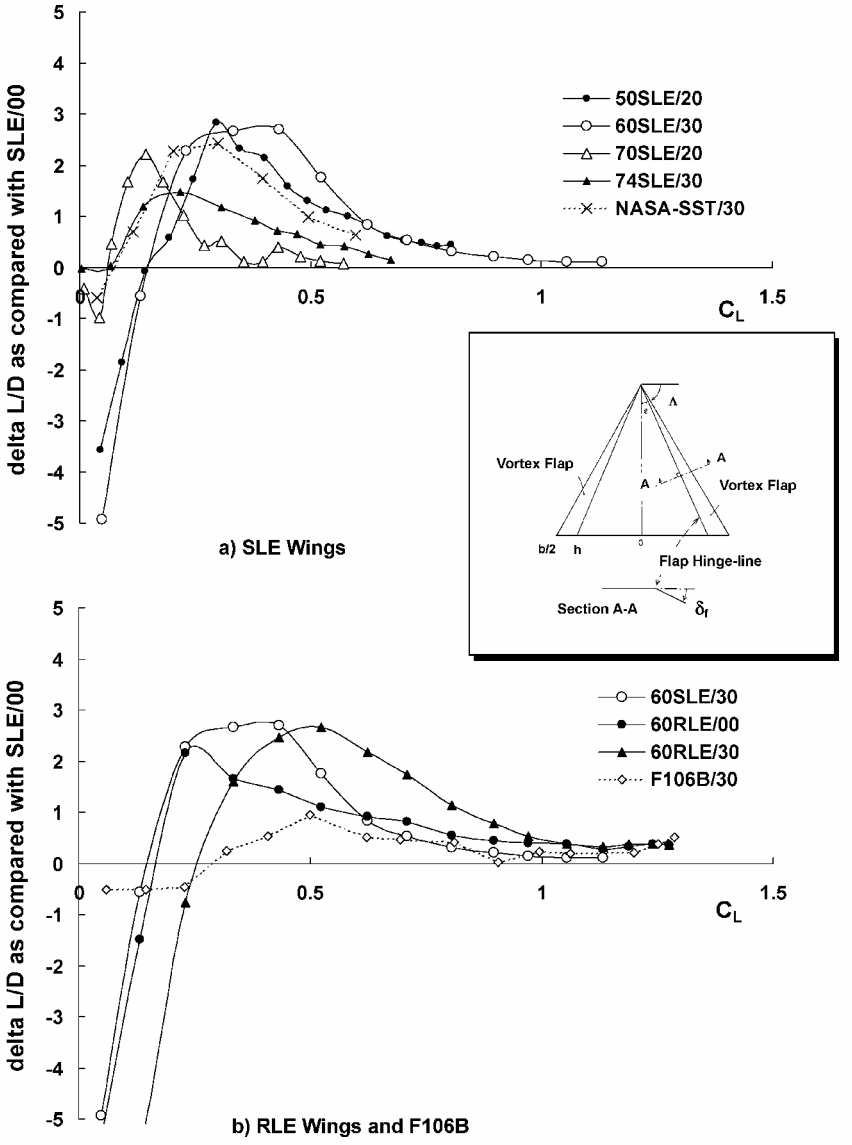

Fig. 1 Actual L/D improvement as compared with SLE/00.

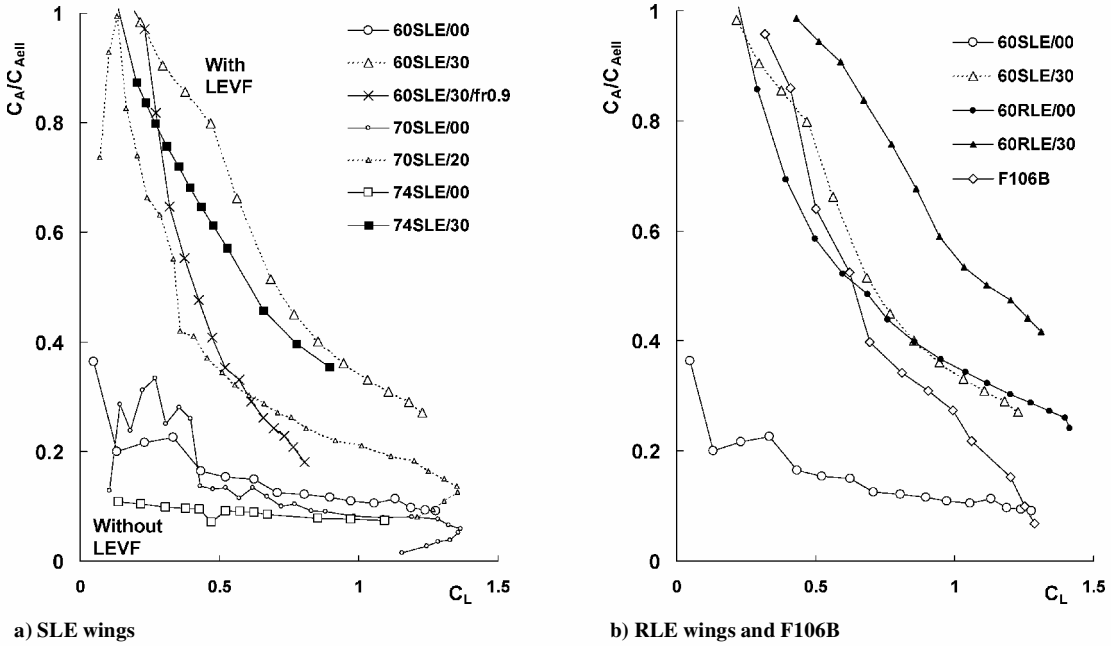

Fig. 2 Attainable thrust ratio C_A/C_{Aell} vs C_L.

where h is the length between the flap hinge line and the wing centerline at the trailing edge and $b/2$ is the semispan length at the trailing edge. For the plain delta wing without vortex flaps, $fr = 1$.

The vortex flap experiments conducted by the present author and coworkers are summarized in Table 1.[6–10] Details of the experiments are given in each reference. Experimental results in Table 1 are used to discuss the vortex flap characteristics in the following sections. Except where noted, most of the experiments were made at $fr = 0.75$ and with sharp leading edges. All aerodynamic coefficients were calculated based on the constant datum delta wing area. Table 1 also summarizes the experimental details of other references[11–13] that are used in this Note. They are for a 74-deg delta wing–body configuration with vortex flaps,[11] a highly swept untwisted uncambered arrow wing SST configuration,[12] and the F106B aircraft model when constant-chord sharp LEVFs are attached to the original 60-deg delta wing.[13]

Table 1 indicates that the measurements were conducted at different Reynolds numbers. However, according to Refs. 14 and 15, it is known that the aerodynamic characteristics of sharp leading-edge delta wings and the behavior of the leading-edge separation vortex are not much affected by differences in either the model cross section or in the Reynolds number. The rounded leading-edge delta wing results should be treated with caution because of the Reynolds number effects.

Examples of the notation used in this note are as follows. The 70-deg sharp leading-edge (SLE) wing with no flap deflection, $\delta_f = 0$ deg is denoted 70SLE/00 and the 60-deg rounded leading edge (RLE) with a flap deflection of $\delta_f = 30$ deg is denoted 60RLE/30. Other abbreviations used are described in Table 1.

L/D Improvement by the LEVF

To visualize the LEVF effect on L/D more clearly, the increase in actual L/D value for 50SLE/20, 60SLE/30, 70SLE/20, 74SLE/30, and NASA-SST/30 wings is compared with each wing when $\delta_f = 0$ deg as shown in Fig. 1a. The flap deflection angle that attains the best performance for each case is chosen and plotted in Fig. 1a. Figure 1a shows that, except for the 70SLE wing, the benefit of the LEVF is seen in the C_L range between about 0.2 and 0.5. An increase in L/D of about 2–3 can be expected in general over a wide C_L range by deflecting the LEVF.

Figure 1b shows the results of actual L/D value increase in L/D for 60SLE/30, 60RLE/00, 60RLE/30, and F106B/30 wings. The maximum L/D benefit in actual value for the RLE is between 2 and 3, which is almost the same benefit as attained by the SLE LEVFs (Fig. 1a). The significance of the rounded LEVF is that the benefit is still observed at a lift coefficient C_L greater than 0.5, as was discussed in Ref. 10. The RLE without flap deflection (60RLE/00) also indicates some L/D benefit, as discussed in Ref. 16. Because vortex flaps were attached to the leading edge of the original wing of F106B, the C_L of F106B/30 is normalized by the increased wing area and plotted in Fig. 1b. The benefit to F106B/30 is not so high as compared with F106B (no LEVF deflected), which will be discussed again in the next section.

Attainable Thrust Ratio

Figure 2 shows the attainable thrust ratio $C_A/C_{A\,\mathrm{ell}}$ vs C_L curves to discuss the leading-edge suction recovered by the LEVF. $C_A/C_{A\,\mathrm{ell}}$ is defined by

$$\frac{C_A}{C_{A\,\mathrm{ell}}} = \left(\frac{(C_D - C_{D\,\min})\cos\alpha - C_L \sin\alpha}{\left(C_L^2/\pi AR\right)\cos\alpha - C_L \sin\alpha} \right) \tag{2}$$

where $C_{D\,\min}$ is the minimum C_D. This expression[3] shows the measured axial force divided by the theoretical maximum axial force, that is, that for a wing with elliptic spanwise loading. This parameter ranges between 0 (no thrust) and 1 (full thrust).

Figure 2a shows results for 60-, 70-, and 74-deg SLE delta wings with and without flap deflection,[6,7,11] together with the 60-deg, sharp delta wing when $\delta_f = 30$ deg and $fr = 0.9$ (60SLE/30/fr0.9) (Ref. 9). Figure 2a shows that the attainable thrust ratio is very

Table 1 Experimental details

Configuration	Λ, deg	LE	LEVF	fr	Cross section	Thickness ratio, %	δ_f, deg	Re	Measurements: Forces	Measurements: Pressure	Measurements: Visualization	Wind tunnel, m	Ref.
60SLE/00	60	Sharp	Tapered	0.75	Convex section	4.8	0–60	2×10^6[a]	6 Components	Surface	——	2.4×1.8 closed	6
60SLE/30													
70SLE/00	70	Sharp	Tapered	0.75	Beveled edge	3	0–50	1×10^6[a]	6 Components	Surface and 5-hole pitot	Oil flow	2×2 closed	7
70SLE/20													
50SLE/20	50	Sharp	Tapered	0.75	Beveled edge	1.8	0–30	6.7×10^5[a]	3 Components	——	Oil flow	$\phi 2$ open	8
60RLE/00	60	Rounded	Tapered	0.75	Modified convex	4.8	0–60	2×10^6[a]	6 Components	Surface	——	2.4×1.8 closed	10
60RLE/30								3×10^6[a]					
60SLE/30/fr0.9	60	Sharp	Tapered	0.6–0.9	Beveled edge	1.8	0, 30	6.7×10^5[a]	3 Components	——	Oil flow	$\phi 2$Open	9
74SLE/00	74 (at flap hinge line)[b] Delta wing plus fuselage	Sharp	Nearly constant chord	0.755[c]	Beveled edge flat plate	1.6[d]	0, 30, 40, 45	5.4×10^6[e]	6 Components	Surface	——	2.1×3.0 high speed	11
74SLE/30													
NASA-SST/30	$74 + 60$ (Arrow wing)[b] SST configuration	Rounded	Inversely tapered	≈0.85[c]	Coordinate data supplied	Coordinate data supplied	0, 30	4.8×10^6[e]	6 Components	Surface	——	1.2×2.1 closed	12
F106B	60[b]	Attached sharp-edged vortex flat	Constant chord	0.915[c]	Modified NACA0004-65 with conical cambered LE	3.9 at root[d]	0, 30, 40, 50	1.3×10^6[e]	6 Components	——	——	9×18 open	13
F106B/30	0.15-scale F106B												

[a]Based on root chord. [b]At LE. [c]Based on flap area. [d]Thickness ratio t/C_r. [e]Based on mean aerodynamic chord.

low for wings without flap deflection (60SLE/00, 70SLE/00, and 74SLE/00). This comes from that the SLE does not produce any leading-edge suction force. When the vortex flap is deflected, the attainable thrust ratio increases. Almost full thrust is observed when C_L is relatively small. Also as C_L increases, $C_A/C_{A\,\mathrm{ell}}$ decreases for all configurations. These results clearly indicate abilities to recover suction by vortex flaps. Even the vortex flap with a small spanwise length attains a very high suction force (60SLE/30/fr0.9).

Figure 2b shows results for 60-deg RLE delta wings (60RLE/00 and 60RLE/30) (Ref. 10) and F106B (Ref. 13) together with 60-deg sharp delta wing. Figure 2b indicates that the attainable thrust ratio is the highest for 60RLE/30, and benefit of the RLE can be clearly seen at relatively high-lift coefficients (C_L greater than 0.5) (Ref. 10). This means that the high-leading-edge suction force is acting on the RLE as was discussed. The $C_A/C_{A\,\mathrm{ell}}$ distribution of F106B (no LEVF deflected) is relatively similar to those of 60SLE/30 and 60RLE/00. The F106B main wing has a modified NACA0004-65 section with conical cambered leading edge.[17] This means that the wing originally has a kind of drooped RLE that may act like a rounded LEVF. Because of this, there was only a small benefit in L/D between F106B and F106B/30, as was shown in Fig. 1b.

Summary

In summary, the attainable thrust is very low for the sharp-edged wing without the vortex flap deflection. When the vortex flap is deflected, this attainable thrust increases, which clearly indicates the ability to recover the leading-edge suction force by use of the various vortex flap configurations. Even the vortex flap with a small spanwise length attains a very high suction force. The benefit of the sharp-edged vortex flap is attained at a lift coefficient C_L smaller than about 0.5 for most of the cases. However, the L/D is improved at C_L greater than about 0.5 for the tested rounded LEVF attached to the 60-deg delta wing.

Acknowledgments

The author would like to express his gratitude to J. L. Stollery, College of Aeronautics, Cranfield University and R. K. Nangia, Nangia Aero Research Associates for their beneficial advice.

References

[1]Rao, D. M., "Leading Edge Vortex-Flap Experiments on a 74 deg. Delta Wing," NASA CR-159161, Nov. 1979.

[2]Rao, D. M., and Campbell, J. F., "Vortical Flow Management Techniques," *Progress in Aerospace Sciences*, Pergamon Press, Oxford, Vol. 24, No. 3, 1987, pp. 173–224.

[3]Traub, L. W., "Aerodynamic Characteristics of Vortex Flaps on a Double-Delta Planform," *Journal of Aircraft*, Vol. 32, No. 2, 1995, pp. 449, 450.

[4]Levin, D., "Vortex Flaps Canard Configuration for Improved Maneuverability," *Journal of Aircraft*, Vol. 34, No. 5, 1997, pp. 693–695.

[5]Bushnell, D. M., "Longitudinal Vortex Control—Techniques and Applications," *Aeronautical Journal*, Vol. 96, No. 958, 1992, pp. 293–312.

[6]Rinoie, K., and Stollery, J. L., "Experimental Studies of Vortex Flaps and Vortex Plates," *Journal of Aircraft*, Vol. 31, No. 2, 1994, pp. 322–329.

[7]Rinoie, K., Fujita, T., Iwasaki, A., and Fujieda, H., "Experimental Studies of a 70-Degree Delta Wing with Vortex Flaps," *Journal of Aircraft*, Vol. 34, No. 5, 1997, pp. 600–605.

[8]Rinoie, K., "Studies of Vortex Flaps for Different Sweepback Angle Delta Wings," *Aeronautical Journal*, Vol. 101, No. 1009, 1997, pp. 409–416.

[9]Rinoie, K., and Kwak, D. Y., "Studies on Vortex Flaps Having Different Flap Hinge-Line Positions," *Journal of Aircraft*, Vol. 38, No. 2, 2001, pp. 396–398.

[10]Rinoie, K., "Experiments of a 60-Degree Delta Wing with Rounded Leading-Edge Vortex Flaps," *Journal of Aircraft*, Vol. 37, No. 1, 2000, pp. 37–44.

[11]Frink, N. T., "Subsonic Wind-Tunnel Measurements of a Slender Wing-Body Configuration Employing a Vortex Flap," NASA TM-89101, July 1987.

[12]Coe, P. L., Jr., Kjelgaard, S. O., and Gentry, G. L., Jr., "Low-Speed Aerodynamic Characteristics of a Highly Swept, Untwisted, Uncambered Arrow Wing," NASA TP 2176, Oct. 1983.

[13]Yip, L. P., and Murri, D. G., "Wind-Tunnel Free-Flight Investigation of a 0.15-Scale Model of the F106B Airplane with Vortex Flaps," NASA TP 2700, May 1987.

[14]Rom, J., *High Angle of Attack Aerodynamics*, Springer-Verlag, NewYork, 1991, pp. 15–21.

[15]Kegelman, J., and Roos, F., "Effects of Leading-Edge Shape and Vortex Burst on the Flowfield of a 70 Degree Sweep Delta-Wing," AIAA Paper 89-0086, Jan. 1989.

[16]Traub, L. W., "Comparative Study of Delta Wings with Blunt Leading Edges and Vortex Flaps," *Journal of Aircraft*, Vol. 33, No. 4, 1996, pp. 828–830.

[17]DiCarlo, D. J., Brown, P. W., and Hallissy, J. B., "Flight Test Operations Using an F-106B Research Airplane Modified with a Wing Leading-Edge Vortex Flap," AIAA Paper 92-4094, Aug. 1992.